JOURNAL OF THEORETICAL
AND APPLIED MECHANICS
52, 3, pp. 617-628, Warsaw 2014

THERMAL STRESSES AROUND TWO UPPER CRACKS PLACED SYMMETRICALLY ABOUT A LOWER CRACK IN AN INFINITE ORTHOTROPIC PLANE UNDER UNIFORM HEAT FLUX

Shouetsu Itou

Kanagawa University Rokkakubashi, Department of Mechanical Engineering, Kanagawa-ku, Yokohama, Japan
e-mail: itous001@kanagawa-u.ac.jp

Two upper collinear cracks are placed parallel to a lower crack in an infinite orthotropic plane under uniform heat flux perpendicular to the cracks. The surfaces of the cracks are assumed to be thermally insulated. The mixed boundary value conditions with respect to the temperature field and those with respect to the stress field are reduced to dual integral equations using the Fourier transform technique. In order to satisfy the boundary conditions outside the cracks, the differences in temperature and displacement at each crack surface are expanded in a series of functions that are zero outside the cracks. The unknown coefficients in each series are evaluated using the Schmidt method. The stress intensity factors are then calculated numerically for selected crack configurations.

Keywords: heat flux, three parallel cracks, stress intensity factor, infinite orthotropic plane

1. Introduction

Fiber-reinforced composite materials have been widely used as structural members in airplanes, automobiles and high-speed trains because they are both strong and lightweight. In their construction, a matrix is reinforced with fibers, which are stiffer and stronger than the matrix. Therefore, it follows that the composite materials are orthotropic. When the materials are subjected to repeated cycles of stress, some cracks may develop in the matrix material because the fibers are stronger than the matrix. If cracked composite materials are used in high-temperature or low-temperature environments, heat flows through the materials. In this case, it is useful to evaluate the stress intensity factors that are caused by the disturbance in heat flux around the cracks.

The stress intensity factor was first determined for a crack in an infinite plate in which heat flowed perpendicular to the crack by Sih (1962). Later, Sekine (1977) evaluated the stress intensity factor for a crack in a half-plane under heat flux. Sekine (1979) also determined the thermal stresses for two cracks in an infinite plate under heat flux. The two cracks were situated arbitrarily in the infinite plate, and heat flowed perpendicular to one of the two cracks (Sekine, 1979). Itou (1991) evaluated the thermal stresses for a crack in an infinite elastic layer the upper surface of which was heated to maintain a constant temperature T_0, and the lower surface of which was cooled to maintain a constant temperature $-T_0$. Itou and Rengen (1993) evaluated the thermal stresses around two parallel cracks in two bonded dissimilar elastic half-planes the upper crack of which lied in the upper half-plane, while the other crack was in the lower half-plane. The stress intensity factors were obtained for a crack in an adhesive layer sandwiched between two dissimilar elastic half-planes under heat flux perpendicular to the cracks by Itou (1993). Later, a similar problem was also solved for the case in which two collinear cracks were situated in the adhesive layer sandwiched between two dissimilar elastic half-planes by Itou and Rengen (1995).

As for orthotropic elastic problems that are related to thermal stresses, Tsai (1994) determined the stress intensity factors for a crack in an infinite orthotropic plate under uniform heat flow. Chen and Zhang (1988) evaluated stress intensity factors around two collinear cracks in an orthotropic plate under heat flux. Later, Chen and Zhang (1994, 1995) evaluated stress intensity factors caused by a disturbance in heat flux from three coplanar cracks in an infinite orthotropic plate. The stress intensity factors were also evaluated for two parallel cracks in an infinite orthotropic plate under heat flux by Itou (2001).

The solutions for an infinite plate are ineffective if a crack exists near the plane surface of a structural member. Chen and Zhang (1993) determined the thermal stresses around two collinear cracks in an orthotropic strip. In their solution, two cracks were placed in the middle surface of the strip. If the cracks were situated near the stress-free surface, the thermal stress intensity factors would have been affected by the presence of the surface. Itou (2000) estimated the stress intensity factors around a crack in an orthotropic layer the upper surface of which maintained a constant temperature T_0, while the lower surface maintained a constant temperature $-T_0$. In the paper by Itou (2000) the stress intensity factors were also determined for a crack under heat flux.

Since stresses around a crack are very high, a parallel crack may also develop above the original crack in composite materials. If a tensile stress is applied to the material, a stress increase and stress shielding occur around the crack ends due to the position of the upper cracks (Kamei and Yokobori, 1974). It is necessary to clarify whether or not the same phenomenon also occurs in a cracked orthotropic material under heat flux. In the present paper, the thermal stresses around three insulated cracks in an infinite orthotropic plate are evaluated under heat flux. Two upper cracks are situated symmetrically on either side of the central crack, and heat flows perpendicular to the cracks. The mixed boundary value conditions concerning the temperature field are reduced to two pairs of dual integral equations. To solve the equations, the differences in temperature at each crack surface are expanded in a series of functions that are zero outside the cracks. The unknown coefficients in the series are determined from the conditions inside the cracks using the Schmidt method (Yau, 1967). Next, the mixed boundary value conditions concerning the stress field are reduced to a set of dual integral equations. The differences in displacement at the upper and lower cracks are also expanded in a series of functions that are zero outside the cracks. The Schmidt method is used to solve for the unknown coefficients so as to satisfy the conditions inside the cracks, and the stress expressions are represented by infinite integrals. From the character of the integrands, the stress intensity factors are defined in the usual manner and are computed for steel and ceramic-fiber-reinforced ceramic (Tyrannohex) infinite planes.

2. Fundamental equations

With respect to rectangular coordinates (x, y), as shown in Fig. 1, a crack is situated along the x-axis from $-c$ to c at $y = -h$, and two collinear cracks are situated along the x-axis from $-b$ to $-a$ and from a to b at $y = 0$. For convenience, we refer to $-h \leqslant y \leqslant 0$ as layer (1), $0 \leqslant y$ as upper half-plane (2), and $y \leqslant -h$ as lower half-plane (3).

The fundamental equations for an orthotropic material were derived by Nowinski (1978). For convenience, the basic equations are shown here. If a state of plane stress is assumed, the stresses can be expressed by

$$\tau_{xx} = Q_{11}\varepsilon_{xx} + Q_{12}\varepsilon_{yy} - \beta_1 T \qquad \tau_{yy} = Q_{12}\varepsilon_{xx} + Q_{22}\varepsilon_{yy} - \beta_2 T \qquad \tau_{xy} = Q_{66}\gamma_{xy} \tag{2.1}$$

with

$$Q_{11} = \frac{E_{xx}}{1-\nu_{yx}\nu_{xy}} \qquad Q_{22} = \frac{E_{yy}}{1-\nu_{yx}\nu_{xy}} \qquad Q_{12} = \frac{E_{yy}\nu_{xy}}{1-\nu_{yx}\nu_{xy}} = \frac{E_{xx}\nu_{yx}}{1-\nu_{yx}\nu_{xy}}$$
$$Q_{66} = G_{xy} \qquad \beta_1 = Q_{12}\alpha_{yy} + Q_{11}\alpha_{xx} \qquad \beta_2 = Q_{12}\alpha_{xx} + Q_{22}\alpha_{yy} \tag{2.2}$$

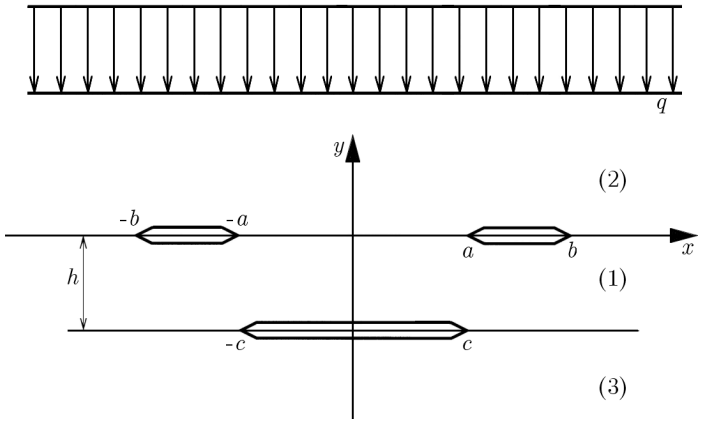

Fig. 1. Coordinate system and three parallel cracks

where E_{xx}, E_{yy} are Young's moduli, G_{xy} is the shear modulus, ν_{xy}, ν_{yx} are Poisson's ratios, and α_{xx}, α_{yy} are the coefficients of linear expansion. The relationships between the strains and displacements are given as follows

$$\varepsilon_{xx} = \frac{\partial u}{\partial x} \qquad \varepsilon_{yy} = \frac{\partial v}{\partial y} \qquad \gamma_{xy} = \frac{\partial u}{\partial y} + \frac{\partial v}{\partial x} \tag{2.3}$$

In equation (2.1), the temperature T satisfies

$$\frac{\partial^2 T}{\partial x^2} + k^2 \frac{\partial^2 T}{\partial y^2} = 0 \tag{2.4}$$

with

$$k^2 = \frac{k_y}{k_x} \tag{2.5}$$

where k_y, k_x are the thermal conductivities.

Substituting equation (2.1) into the equations of equilibrium for the forces reduces these equations to the forms

$$\begin{aligned} Q_{11}\frac{\partial^2 u}{\partial x^2} + Q_{66}\frac{\partial^2 u}{\partial y^2} + L\frac{\partial^2 v}{\partial x \partial y} - \beta_1 \frac{\partial T}{\partial x} = 0 \\ Q_{66}\frac{\partial^2 v}{\partial x^2} + Q_{22}\frac{\partial^2 v}{\partial y^2} + L\frac{\partial^2 u}{\partial x \partial y} - \beta_2 \frac{\partial T}{\partial y} = 0 \end{aligned} \tag{2.6}$$

with

$$L = Q_{12} + Q_{66} \tag{2.7}$$

3. Boundary conditions

Uniform heat flow (heat flux) q is applied perpendicular to the three cracks as shown in Fig. 1. Stresses are caused when the heat flow is disturbed by the insulating effect of the cracks. The temperature field can be provided using the following boundary conditions

$$\frac{\partial T_1}{\partial y} = \begin{cases} \dfrac{\partial T_2}{\partial y} & \text{at} \quad y = 0, \quad |x| \leqslant \infty \\ -t & \text{at} \quad y = 0, \quad a \leqslant |x| \leqslant b \\ \dfrac{\partial T_3}{\partial y} & \text{at} \quad y = -h, \quad |x| \leqslant \infty \\ -t & \text{at} \quad y = -h, \quad 0 \leqslant |x| \leqslant c \end{cases} \tag{3.1}$$

$$T_1 = \begin{cases} T_2 & \text{at} \quad y = 0, \quad 0 \leqslant |x| \leqslant a, \quad b \leqslant |x| \leqslant \infty \\ T_3 & \text{at} \quad y = -h, \quad c \leqslant |x| \leqslant \infty \end{cases} \tag{3.2}$$

with

$$t = \frac{q}{k_{y1}} \tag{3.3}$$

The variables with the subscript "1" are for layer (1). The variables for upper half-plane (2) and lower half-plane (3) are denoted with the subscripts "2" and "3", respectively.

The stress field can be evaluated using the following boundary conditions

$$\tau_{yy1} = \begin{cases} \tau_{yy2} & \text{at} \quad y = 0, \quad |x| \leqslant \infty \\ 0 & \text{at} \quad y = 0, \quad a \leqslant |x| \leqslant b \\ \tau_{yy3} & \text{at} \quad y = -h, \quad |x| \leqslant \infty \\ 0 & \text{at} \quad y = -h, \quad 0 \leqslant |x| \leqslant c \end{cases} \tag{3.4}$$

$$\tau_{xy1} = \begin{cases} \tau_{xy2} & \text{at} \quad y = 0, \quad |x| \leqslant \infty \\ 0 & \text{at} \quad y = 0, \quad a \leqslant |x| \leqslant b \\ \tau_{xy3} & \text{at} \quad y = -h, \quad |x| \leqslant \infty \\ 0 & \text{at} \quad y = -h, \quad 0 \leqslant |x| \leqslant c \end{cases} \tag{3.5}$$

$$u_1 = \begin{cases} u_2 & \text{at} \quad y = 0, \quad 0 \leqslant |x| \leqslant a, \quad b \leqslant |x| \leqslant \infty \\ u_3 & \text{at} \quad y = -h, \quad c \leqslant |x| \leqslant \infty \end{cases} \tag{3.6}$$

$$v_1 = \begin{cases} v_2 & \text{at} \quad y = 0, \quad 0 \leqslant |x| \leqslant a, \quad b \leqslant |x| \leqslant \infty \\ v_3 & \text{at} \quad y = -h, \quad c \leqslant |x| \leqslant \infty \end{cases} \tag{3.7}$$

4. Analysis

4.1. Fundamental equations in Fourier domain

To find the solutions, the Fourier transforms are introduced as

$$\overline{f}(\xi) = \int_{-\infty}^{\infty} f(x) \exp(\mathrm{i}\xi x)\, dx \qquad f(x) = \frac{1}{2\pi} \int_{-\infty}^{\infty} \overline{f}(\xi) \exp(-\mathrm{i}\xi x)\, d\xi \tag{4.1}$$

Applying equation $(4.1)_1$ to equation (2.6) results in

$$\begin{aligned} Q_{66}\frac{d^2\overline{u}}{dy^2} - \xi^2 Q_{11}\overline{u} - \mathrm{i}L\xi\frac{d\overline{v}}{dy} + \mathrm{i}\beta_1\xi\overline{T} = 0 \\ Q_{22}\frac{d^2\overline{v}}{dy^2} - \xi^2 Q_{66}\overline{v} - \mathrm{i}L\xi\frac{d\overline{u}}{dy} - \beta_2\frac{\partial\overline{T}}{\partial y} = 0 \end{aligned} \tag{4.2}$$

Eliminating $\overline{u}$ or $\overline{v}$ from equation (4.2), the ordinary differential equations are obtained as

$$\begin{aligned}
&\zeta_1\frac{d^4\overline{u}}{dy^4}+\zeta_2\frac{d^2\overline{u}}{dy^2}+\zeta_3\overline{u}=\mathrm{i}\eta_1\frac{d^2\overline{T}}{dy^2}+\mathrm{i}\eta_2\overline{T}\\
&\zeta_1\frac{d^4\overline{v}}{dy^4}+\zeta_2\frac{d^2\overline{v}}{dy^2}+\zeta_3\overline{v}=\eta_3\frac{d^3\overline{T}}{dy^3}+\eta_4\frac{d\overline{T}}{dy}
\end{aligned}\tag{4.3}$$

with

$$\begin{aligned}
&\zeta_1=\frac{Q_{22}Q_{66}}{L} && \zeta_2=-(Q_{66}^2+Q_{11}Q_{22}-L^2)\frac{\xi^2}{L}\\
&\zeta_3=Q_{11}Q_{66}\frac{\xi^4}{L} && \eta_1=\xi\Big(\beta_2-\frac{\beta_1Q_{22}}{L}\Big)\\
&\eta_2=\beta_1Q_{66}\frac{\xi^3}{L} && \eta_3=\frac{Q_{66}\beta_2}{L} \qquad \eta_4=\xi^2\Big(\beta_1-\frac{\beta_2Q_{11}}{L}\Big)
\end{aligned}\tag{4.4}$$

The Fourier-transformed stresses are found to be

$$\begin{aligned}
&\overline{\tau}_{xx}=Q_{11}(-\mathrm{i}\xi)\overline{u}+Q_{12}\frac{d\overline{v}}{dy}-\beta_1\overline{T} \qquad \overline{\tau}_{yy}=Q_{12}(-\mathrm{i}\xi)\overline{u}+Q_{22}\frac{d\overline{v}}{dy}-\beta_2\overline{T}\\
&\overline{\tau}_{xy}=Q_{66}\frac{d\overline{u}}{dy}-\mathrm{i}\xi Q_{66}\overline{v}
\end{aligned}\tag{4.5}$$

Equation (2.4) can now be expressed in the Fourier domain as

$$\frac{d^2\overline{T}}{dy^2}-\Big(\frac{\xi}{k}\Big)^2\overline{T}=0\tag{4.6}$$

4.2. Temperature field

The solutions for equation (4.6) have the following forms for layer (1), upper half-plane (2), and lower half-plane (3), respectively

$$\begin{aligned}
&\overline{T}_1=A_1\sinh\frac{|\xi|y}{k}+B_1\cosh\frac{|\xi|y}{k} \qquad \overline{T}_2=A_2\exp\Big(-\frac{|\xi|y}{k}\Big)\\
&\overline{T}_3=A_3\exp\Big(\frac{|\xi|y}{k}\Big)
\end{aligned}\tag{4.7}$$

where A_1, B_1, A_2, and A_3 are unknown coefficients. Boundary conditions $(3.1)_{1,3}$, which are valid for $-\infty<x<+\infty$, can be easily satisfied. In order to satisfy equations (3.2), the temperatures at $y=0$ and $y=-h$ are expanded by the series

$$\begin{aligned}
&\pi(T_1^0-T_2^0)=\begin{cases}\displaystyle\sum_{n=1}^{\infty}c_n\frac{1}{2n}\sin\Big[n\sin^{-1}\Big(\frac{a+b-2|x|}{b-a}\Big)-\frac{n\pi}{2}\Big] & \text{for} \quad a\leqslant|x|\leqslant b\\ 0 & \text{for} \quad 0\leqslant|x|\leqslant a,\ b\leqslant|x|\leqslant\infty\end{cases}\\
&\pi(T_1^{-h}-T_3^{-h})=\begin{cases}\displaystyle\sum_{n=1}^{\infty}c_n'\cos\Big[(2n-1)\sin^{-1}\frac{x}{c}\Big] & \text{for} \quad 0\leqslant|x|\leqslant c\\ 0 & \text{for} \quad c\leqslant|x|\leqslant\infty\end{cases}
\end{aligned}\tag{4.8}$$

where c_n and c_n' are the unknown coefficients, and the superscripts "0" and "$-h$" denote the values at $y=0$ and $y=-h$, respectively. The Fourier transforms of equations (4.8) can be expressed by

$$\begin{aligned}
&\overline{T}_1^0 - \overline{T}_2^0 = \sum_{n=1}^{\infty} c_n \frac{1}{\xi} \sin\Big[\frac{(a+b)\xi}{2} - \frac{n\pi}{2}\Big] J_n\Big[\frac{(b-a)\xi}{2}\Big] \\
&\overline{T}_1^{-h} - \overline{T}_3^{-h} = \sum_{n=1}^{\infty} c'_n \frac{(2n-1)}{\xi} J_{2n-1}(c\xi)
\end{aligned} \tag{4.9}$$

where $J_n(\xi)$ is the Bessel function. Then, it can be easily shown that remaining boundary conditions (3.2) and (3.5) are reduced to the forms

$$\begin{aligned}
&\sum_{n=1}^{\infty} c_n E_n(x) + \sum_{n=1}^{\infty} c'_n F_n(x) = -t \qquad \text{for} \quad a \leqslant x \leqslant b \\
&\sum_{n=1}^{\infty} c_n G_n(x) + \sum_{n=1}^{\infty} c'_n H_n(x) = -t \qquad \text{for} \quad 0 \leqslant x \leqslant c
\end{aligned} \tag{4.10}$$

where the expressions of the known functions $E_n(x)$, $F_n(x)$, $G_n(x)$, and $H_n(x)$ are omitted. Now, equation (4.10) can be solved for the unknown coefficients c_n and c'_n using the Schmidt method (Yau, 1967). Here, the temperature has been determined completely.

4.3. Stress field

Next, the stress field is evaluated. It can be seen that the solutions to equation (4.3) take the following forms for i $(i = 1, 2, 3)$

$$\begin{aligned}
\overline{u}_1 &= C_1 \sinh(\alpha_1 y) + D_1 \cosh(\alpha_1 y) + E_1 \sinh(\alpha_2 y) + F_1 \cosh(\alpha_2 y) \\
&\quad + \mathrm{i}A_1 \frac{f_1}{\xi} \sinh\Big(\frac{|\xi| y}{k}\Big) + \mathrm{i}B_1 \frac{f_1}{\xi} \cosh\Big(\frac{|\xi| y}{k}\Big) \\
\overline{v}_1 &= \mathrm{i}\gamma_1 D_1 \sinh(\alpha_1 y) + \mathrm{i}\gamma_1 C_1 \cosh(\alpha_1 y) + \mathrm{i}\gamma_2 F_1 \sinh(\alpha_2 y) + \mathrm{i}\gamma_2 E_1 \cosh(\alpha_2 y) \\
&\quad + B_1 \frac{f_2}{|\xi|} \sinh\Big(\frac{|\xi| y}{k}\Big) + A_1 \frac{f_2}{|\xi|} \cosh\Big(\frac{|\xi| y}{k}\Big) \\
\overline{u}_2 &= C_2 \exp(-\alpha_1 y) + E_2 \exp(-\alpha_2 y) - \mathrm{i}A_1 \frac{f_1}{\xi} \exp\Big(-\frac{|\xi| y}{k}\Big) \\
\overline{v}_2 &= -\mathrm{i}\gamma_1 C_2 \exp(-\alpha_1 y) - \mathrm{i}\gamma_2 E_2 \exp(-\alpha_2 y) + A_1 \frac{f_2}{|\xi|} \exp\Big(-\frac{|\xi| y}{k}\Big) \\
\overline{u}_3 &= C_3 \exp(\alpha_1 y) + E_3 \exp(\alpha_2 y) + \mathrm{i}A_1 \frac{g_1 f_1}{\xi} \exp\Big(\frac{|\xi| y}{k}\Big) + \mathrm{i}B_1 \frac{g_2 f_1}{\xi} \exp\Big(\frac{|\xi| y}{k}\Big) \\
\overline{v}_3 &= -\mathrm{i}\gamma_1 C_3 \exp(\alpha_1 y) + \mathrm{i}\gamma_2 E_3 \exp(\alpha_2 y) \\
&\quad + A_1 \frac{g_1 f_2}{|\xi|} \exp\Big(\frac{|\xi| y}{k}\Big) + B_1 \frac{g_2 f_2}{|\xi|} \exp\Big(\frac{|\xi| y}{k}\Big)
\end{aligned} \tag{4.11}$$

where C_i, D_i, E_i, and F_i are unknown coefficients, and α_1 and α_2 are the roots of the following equation

$$\zeta_1 \alpha^4 + \zeta_2 \alpha^2 + \zeta_3 = 0 \tag{4.12}$$

In equations (4.11), γ_1, γ_2, f_1, f_2, g_1, and g_2 are expressed by

$$\begin{aligned}
&\gamma_1 = \frac{\xi^2 Q_{11} - Q_{66}\alpha_1^2}{L\xi\alpha_1} \qquad \gamma_2 = \frac{\xi^2 Q_{11} - Q_{66}\alpha_2^2}{L\xi\alpha_2} \\
&f_1 = \frac{[\beta_1(Q_{66}k^2 - Q_{22}) + \beta_2 L]k^2}{f_3} \qquad f_2 = \frac{Q_{66}\beta_2 k + k^3(\beta_1 L - Q_{11}\beta_2)}{f_3} \\
&f_3 = Q_{66}Q_{22} - k^2(Q_{66}^2 + Q_{11}Q_{22} - L) + Q_{11}Q_{66}k^4 \\
&g_1 = \frac{\cosh\left(-\frac{|\xi|h}{k}\right)}{\exp\left(-\frac{|\xi|h}{k}\right)} \qquad g_2 = \frac{\sinh\left(-\frac{|\xi|h}{k}\right)}{\exp\left(-\frac{|\xi|h}{k}\right)}
\end{aligned} \tag{4.13}$$

Substituting equations (4.7) and (4.11) into equation (4.5), the stress expressions are obtainable in the Fourier domain. Equations (3.8) and (3.11) are valid in the entire region of x, and these can be easily satisfied.

To satisfy equations (3.10) and (3.13), the differences in displacement at $y = 0$ and at $y = -h$ are expanded in the following series

$$\pi(u_1^0 - u_2^0) = \begin{cases} \sum\limits_{n=1}^{\infty} d_n \frac{1}{2n} \sin\Big[n \sin^{-1}\Big(\frac{a+b-2|x|}{b-a}\Big) - \frac{n\pi}{2}\Big] \operatorname{sgn}(x) & \text{for} \quad a \leqslant |x| \leqslant b \\ 0 & \text{for} \quad \begin{array}{l} 0 \leqslant |x| \leqslant a, \\ b \leqslant |x| \leqslant \infty \end{array} \end{cases}$$

$$\pi(v_1^0 - v_2^0) = \begin{cases} \sum\limits_{n=1}^{\infty} e_n \frac{1}{2n} \sin\Big[n \sin^{-1}\Big(\frac{a+b-2|x|}{b-a}\Big) - \frac{n\pi}{2}\Big] & \text{for} \quad a \leqslant |x| \leqslant b \\ 0 & \text{for} \quad \begin{array}{l} 0 \leqslant |x| \leqslant a, \\ b \leqslant |x| \leqslant \infty \end{array} \end{cases}$$

$$\pi(u_1^{-h} - u_3^{-h}) = \begin{cases} \sum\limits_{n=1}^{\infty} d'_n \sin\Big[2n \sin^{-1}\frac{x}{c}\Big] & \text{for} \quad 0 \leqslant |x| \leqslant c \\ 0 & \text{for} \quad c \leqslant |x| \leqslant \infty \end{cases}$$

$$\pi(v_1^{-h} - v_3^{-h}) = \begin{cases} \sum\limits_{n=1}^{\infty} e'_n \cos\Big[(2n-1) \sin^{-1}\frac{x}{c}\Big] & \text{for} \quad 0 \leqslant |x| \leqslant c \\ 0 & \text{for} \quad c \leqslant |x| \leqslant \infty \end{cases} \tag{4.14}$$

where d_n, e_n, d'_n, and e'_n are the unknown coefficients to be determined, and $\operatorname{sgn}(x)$ is the signum function. The Fourier transformed expressions of expressions (4.14) are

$$\begin{aligned}
&\overline{u}_1^0 - \overline{u}_2^0 = -\mathrm{i} \sum_{n=1}^{\infty} d_n \frac{1}{\xi} \cos\Big[\frac{(a+b)\xi}{2} - \frac{n\pi}{2}\Big] J_n\Big[\frac{(b-a)\xi}{2}\Big] \\
&\overline{v}_1^0 - \overline{v}_2^0 = \sum_{n=1}^{\infty} e_n \frac{1}{\xi} \sin\Big[\frac{(a+b)\xi}{2} - \frac{n\pi}{2}\Big] J_n\Big[\frac{(b-a)\xi}{2}\Big] \\
&\overline{u}_1^{-h} - \overline{u}_3^{-h} = \mathrm{i} \sum_{n=1}^{\infty} d'_n \frac{2n}{\xi} J_{2n}(c\xi) \qquad \overline{v}_1^{-h} - \overline{v}_3^{-h} = \sum_{n=1}^{\infty} e'_n \frac{2n-1}{\xi} J_{2n-1}(c\xi)
\end{aligned} \tag{4.15}$$

Then, the stress field can be expressed by the unknown coefficients d_n, e_n, d'_n, and e'_n and the known coefficients c_n and c'_n.

Finally, the remaining boundary conditions inside the cracks are reduced to the following forms:

— for $a \leqslant x \leqslant b$

$$\begin{aligned}
&\sum_{n=1}^{\infty} d_n K_{nu}(x) + \sum_{n=1}^{\infty} e_n L_{nu}(x) + \sum_{n=1}^{\infty} d'_n K_{nu}(x) + \sum_{n=1}^{\infty} e'_n L_{nu}(x) = -U(x) \\
&\sum_{n=1}^{\infty} d_n M_{nu}(x) + \sum_{n=1}^{\infty} e_n N_{nu}(x) + \sum_{n=1}^{\infty} d'_n M_{nu}(x) + \sum_{n=1}^{\infty} e'_n N_{nu}(x) = -V(x)
\end{aligned} \tag{4.16}$$

— for $0 \leqslant x \leqslant c$

$$\begin{aligned}
&\sum_{n=1}^{\infty} d_n K_{nl}(x) + \sum_{n=1}^{\infty} e_n L_{nl}(x) + \sum_{n=1}^{\infty} d'_n K_{nl}(x) + \sum_{n=1}^{\infty} e'_n L_{nl}(x) = -W(x) \\
&\sum_{n=1}^{\infty} d_n M_{nl}(x) + \sum_{n=1}^{\infty} e_n N_{nl}(x) + \sum_{n=1}^{\infty} d'_n M_{nl}(x) + \sum_{n=1}^{\infty} e'_n N_{nl}(x) = -Z(x)
\end{aligned} \tag{4.17}$$

where the expressions of the known functions $K_{nu}(x)$, $L_{nu}(x)$, ..., $W(x)$, and $Z(x)$ are omitted. Equation (4.17) can be solved for the coefficients d_n, e_n, d'_n, and e'_n using the Schmidt method (Itou and Haliding, 1997).

5. Stress intensity factors

Using the relationship for $a \leqslant x$

$$\begin{aligned}
&\int_0^{\infty} J_n(a\xi)\Big[\cos(\xi x),\ \sin(\xi x)\Big]\, d\xi \\
&\quad = \Big[-\frac{a^n}{\sqrt{x^2-a^2}}\Big(x+\frac{1}{\sqrt{x^2-a^2}}\Big)^{-n} \sin\frac{n\pi}{2},\ \frac{a^n}{\sqrt{x^2-a^2}}\Big(x+\frac{1}{\sqrt{x^2-a^2}}\Big)^{-n} \cos\frac{n\pi}{2}\Big]
\end{aligned} \tag{5.1}$$

the stress intensity factors can be determined as follows

$$\begin{aligned}
K_{1a} &= \lim_{x\to a^-} \sqrt{2\pi(a-x)}\tau^0_{yy1} = \sum_{n=1}^{\infty} e_n \frac{-Q^L_4}{\sqrt{2\pi(b-a)}} \\
K_{1b} &= \lim_{x\to b^+} \sqrt{2\pi(x-b)}\tau^0_{yy1} = \sum_{n=1}^{\infty} e_n \frac{(-1)^n Q^L_4}{\sqrt{2\pi(b-a)}} \\
K_{2a} &= \lim_{x\to a^-} \sqrt{2\pi(a-x)}\tau^0_{xy1} = \sum_{n=1}^{\infty} d_n \frac{Q^L_9}{\sqrt{2\pi(b-a)}} \\
K_{2b} &= \lim_{x\to b^+} \sqrt{2\pi(x-b)}\tau^0_{xy1} = \sum_{n=1}^{\infty} d_n \frac{(-1)^{n+1} Q^L_9}{\sqrt{2\pi(b-a)}} \\
K_{1c} &= \lim_{x\to c^+} \sqrt{2\pi(x-c)}\tau^{-h}_{yy1} = \sum_{n=1}^{\infty} e'_n \frac{(1-2n)(-1)^n Q^L_{18}}{\sqrt{\pi c}} \\
K_{2c} &= \lim_{x\to c^+} \sqrt{2\pi(x-c)}\tau^{-h}_{xy1} = \sum_{n=1}^{\infty} d'_n \frac{2n(-1)^n Q^L_{23}}{\sqrt{\pi c}}
\end{aligned} \tag{5.2}$$

where the expressions of the known constants Q^L_4, Q^L_9, Q^L_{18}, and Q^L_{23} are omitted.

6. Numerical examples

The effect of orthotropy on the stress intensity factors can be illustrated by examining Tyrannohex as the orthotropic material. Tyrannohex is a ceramic-fiber-reinforced ceramic material developed by Ishikawa, Kajii, Matsunaga, Hogami, Kohtoku and Nagasawa (1998) and its material properties are listed in Table 1.

Table 1. Material properties

Constants	Steel	Tyrannohex
E_{xx} [GPa]	205.9	135.0
E_{yy} [GPa]	205.9	87.0
μ_{xy} [GPa]	79.2	50.0
ν_{xy}	0.3	0.15
ν_{yx}	$0.3 \cdot 1.01$	0.09667
α_{xx} [$\times 10^{-5}$/°C]	1.14	0.32
α_{yy} [$\times 10^{-5}$/°C]	1.14	0.32
k_x [W/(m°C]	48.6	3.08
k_y [W/(m°C]	48.6	3.08

For an isotropic material, it holds that

$$E_{xx} = E_{yy} \qquad \nu_{xy} = \nu_{yx} \qquad \alpha_{xx} = \alpha_{yy} \qquad k_x = k_y \tag{6.1}$$

This case presents no problems in solving the temperature field. However, equation (4.12) has two kinds of multiple roots. Therefore, equations (4.11) cannot be used as the solution for equation (4.3). The analysis presented here holds, even for an isotropic material, if the value of ν_{yx} is replaced by a value slightly larger than ν_{xy}. In this example, steel is selected as a representative isotropic material, and the constants used for the calculation are also given in Table 1.

The known functions $F_n(x)$ and $G_n(x)$ in equation (4.10) and $K_{nu}(x)$, $L_{nu}(x)$, ..., $N_{nl}(x)$, and $Z(x)$ in equation (4.17) contain semi-infinite integrals with respect to the integral variable ξ. If the integrands of the integrals do not decrease rapidly, these are modified so as to decay rapidly as ξ increases. Then, numerical integration can be performed precisely using Filon's method.

First, the Schmidt method is applied to solve for the coefficients c_n and c'_n in equation (4.10) by taking the first 12 terms in an infinite series. Next, the coefficients d_n, e_n, d'_n, and e'_n in equation (4.17) are solved for. It has been verified that the left-hand side of equation (4.10) coincides with the right-hand side of equation (4.10). The same applies to equation (4.17).

The length of the upper two cracks is fixed to $b - a = c$. The stress intensity factors for steel are calculated numerically against a/c. The results for $h/c = 0.5$, 1.0, and 2.0 are plotted in Figs. 2a, 2b, and 2c, respectively. In these figures, the stress intensity factors are divided by $E_{xx}\alpha_{xx}\sqrt{\pi c^3}t/4$ to show the values as non-dimensional quantities. The stress intensity factors for Tyrannohex are also plotted in Figs. 3a through 3c.

7. Discussion

It is clear that, at the least, one of the values of K_{1a}, K_{1b}, and K_{1c} is negative. Therefore, the crack surfaces come into contact with each other at one or more of the crack ends. In this case, the boundary conditions with respect to the temperature field fail to be valid. The same applies to the boundary conditions with respect to the stress field. In the present paper, it is assumed that the crack surfaces do not come into contact with each other due to the existence of a thin gap.

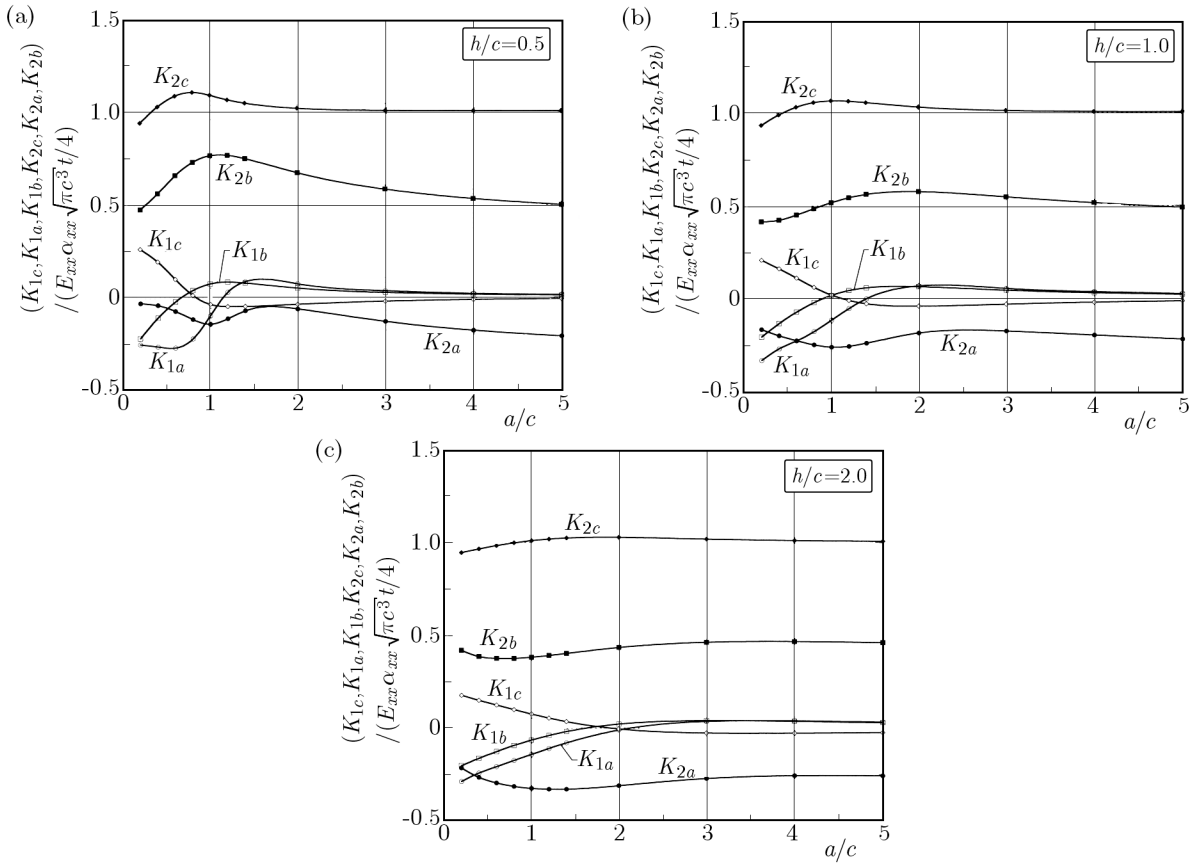

Fig. 2. Stress intensity factors versus a/c for $h/c = 0.5$ (a), $h/c = 1.0$ (b), $h/c = 2.0$ (c) and $b - a = c$ (steel)

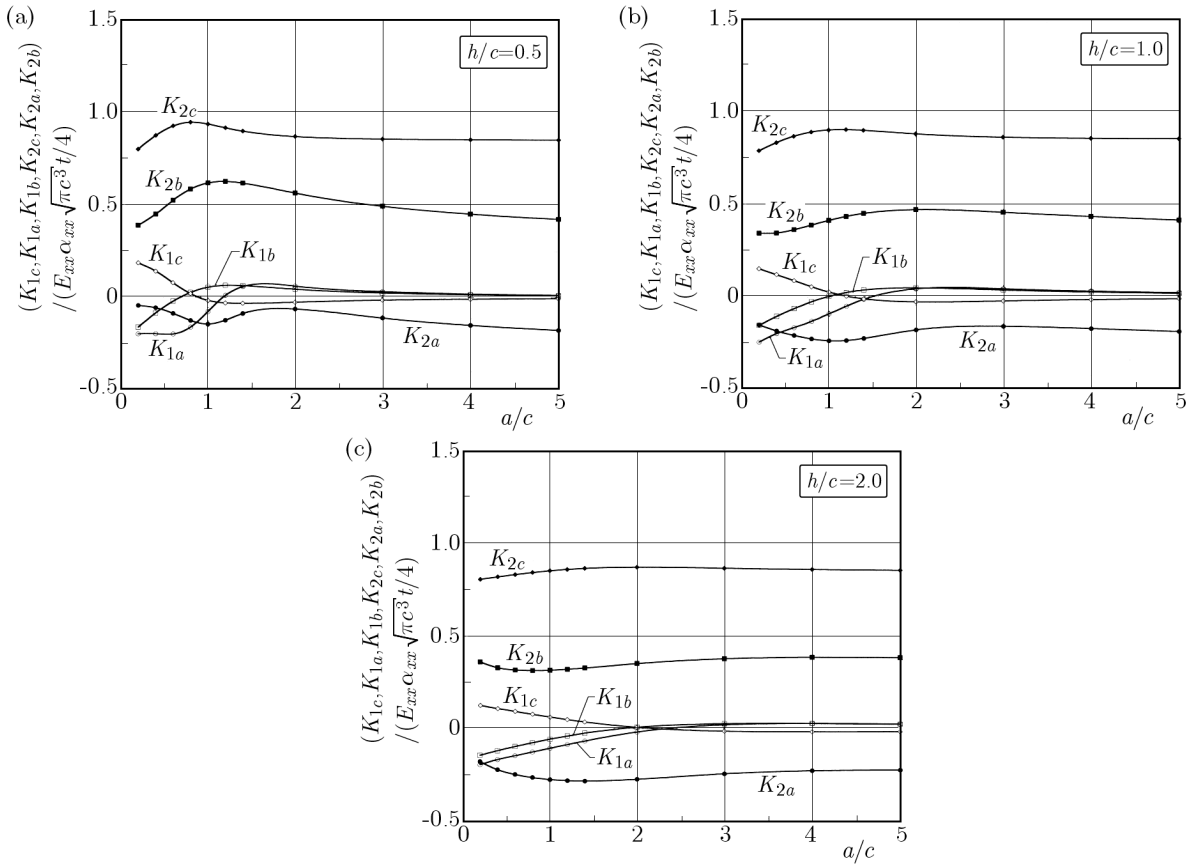

Fig. 3. Stress intensity factors versus a/c for $h/c = 0.5$ (a), $h/c = 1.0$ (b), $h/c = 2.0$ (c) and $b - a = c$ (Tyrannohex)

8. Conclusions

Based on the numerical calculations outlined above, we can draw the following conclusions:

- It is clear that the values of K_{2c} are not affected by the presence of the upper parallel cracks for a value larger than $h/c = 2.0$. However, if the value of h/a decreases, the stress intensity factor K_{2c} appears to increase. For $h/c = 0.5$, the peak value of K_{2c} occurs near $a/c = 0.8$, and stress shielding occurs for $a/c \leqslant 0.3$. In the present paper, the stress intensity factors for $h/c < 0.5$ were not successfully calculated. However, it can probably be estimated that a severe increase in the stresses occurs if h/c decreases.
- For $h/c = 2.0$, the lowest value of K_{2b} appears near $a/c = 0.8$. However, the value of K_{2b} has a large value near $a/c = 1.0$ for $h/c = 0.5$. Therefore, it can be estimated that the value of K_{2b} can be very large if h/c decreases.
- The values of K_{2c} for Tyrannohex are somewhat smaller than those for steel, and the curves for Tyrannohex are similar to those for steel. Therefore, the safety of the cracked structural member will be ensured by comparing the fracture toughness value of Tyrannohex with the values obtained from the curves for steel.

References

1. Chen B., Zhang X., 1988, Thermoelasticity problem of an orthotropic plate with two collinear cracks, *International Journal of Fracture*, **38**, 161-192
2. Chen B., Zhang X., 1993, On plane thermoelasticity problem of an orthotropic strip with two collinear cracks, *Journal of Northwestern Polytechnical University*, **11**, 121-126
3. Chen B., Zhang X., 1994, Orthotropic thermoelasticity problem of symmetrical heat flow disturbed by three coplanar cracks, *International Journal of Fracture*, **67**, 301-314
4. Chen B., Zhang X., 1995, Orthotropic thermoelasticity problem of an antisymmetric heat flow disturbed by three coplanar cracks, *International Journal of Fracture*, **70**, 267-273
5. Ishikawa T., Kohtoku Y., Kumagawa K., Yamamura T., Nagasawa T., 1998, High-strength alkali-resistant sintered SiC fibre stable to 2,200°C, *Nature*, **391-6669**, 773-775
6. Itou S., 1991, Thermal stresses around an isolated crack in an infinite elastic layer (in Japanese), *Transaction of Japan Society of Mechanical Engineers*, **57**, 1752-1758
7. Itou S., 1993, Thermal stresses around a crack in an adhesive layer between two dissimilar elastic half-planes, *Journal of Thermal Stresses*, **16**, 373-400
8. Itou S., 2000, Thermal stress intensity factors of an infinite orthotropic layer with a crack, *International Journal of Fracture*, **103**, 279-291
9. Itou S., 2001, Thermal stresses around two parallel cracks in an infinite orthotropic plate under uniform heat flow, *Journal of Thermal Stresses*, **24**, 677-694
10. Itou S., Haliding H., 1997, Dynamic stress intensity factors around two parallel cracks in an infinite orthotropic plane subjected to incident harmonic stress waves, *International Journal of Solids and Structures*, **34**, 1145-1165
11. Itou S., Rengen Q., 1993, Thermal stresses around two parallel cracks in two bonded dissimilar elastic half-planes, *Archive of Applied Mechanics*, **63**, 377-385
12. Itou S., Rengen Q., 1995, Thermal stresses around two collinear Griffith cracks in an adhesive layer between two dissimilar elastic half-planes, *Journal of Thermal Stresses*, **18**, 185-196
13. Kamei A., Yokobori T., 1974, Some results on stress intensity factors of the cracks and/or slip bands system, Reports of Research Institute of Strength and Fracture of Materials, Tohoku University, **10**, 29-93

14. Nowinski J.L., 1978, *Theory of Thermoelasticity with Applications*, Sijthoff and Noordhoff, The Netherlands

15. Sekine H., 1977, Thermal stresses near tips of an insulated line crack in semi-infinite medium under uniform heat flow, *Engineering Fracture Mechanics*, **9**, 499-507

16. Sekine H., 1979, Thermoelastic interaction between two neighboring cracks (in Japanese), *Transaction of Japan Society of Mechanical Engineers*, **45**, 1058-1063

17. Sih G.C., 1962, On the singular character of thermal stresses near a crack, *ASME Journal of Applied Mechanics*, **29**, 587-589

18. Tsai Y.M., 1984, Orthotropic thermoelastic problem of uniform heat flow disturbed by a central crack, *Journal of Composite Materials*, **18**, 122-131

19. Yau W.F., 1967, Axisymmetric slipless indentation of an infinite elastic cylinder, *SIAM Journal on Applied Mathematics*, **15**, 219-227

Manuscript received October 21, 2013; accepted for print January 16, 2014